2 Background knowledge

This chapter summarizes the basic scientific knowledge necessary for understanding the studies performed in this work. First, the Sun's origin, inner structure, atmosphere and sphere of influence, the heliosphere, are described. Then, the Sun's dynamics with its differential rotation and magnetic field generation are outlined. Further, the solar activity cycle is described, including the meridional flow circulation, appearance of active regions, the surface magnetic field change, and sunspot cycles. The heliospheric magnetic field is depicted from its photospheric emergence in magnetic bright points and coronal superradial expansion, through the formation of the heliospheric current sheet and the Parker spiral to the heliosheath. The solar wind and its properties, the origins of slow and fast streams, stream interaction regions, and coronal mass ejections are described. Furthermore, space weather, solar influence on Earth, the magnetosphere, solar wind-magnetosphere coupling, and geomagnetic indices are portrayed.

2.1 The Sun

13.8 billion years ago the Big Bang formed our universe. The energy density of our universe consists of 69.1 % dark energy, 25.9 % dark matter and 4.9 % baryonic matter, according to calculations using the inflationary ΛCDM[1] cosmology together with the latest cosmic microwave background temperature measurements (Planck Collaboration et al. 2016). After a few minutes the primordial nucleosynthesis left the universe in a state where the baryonic matter was composed of 75.33 %[2] hydrogen, 24.67 % helium and traces of deuterium, tritium and lithium (Planck Collaboration et al. 2016).

Over millions of years this gas cooled down and gravitationally accreted into molecular clouds and formed stars. The first generations of stars (Population III) fused this gas to heavier elements (metals) and supernovae distributed them into space as a foundation for the formation of new stars of low and high metallicity (Population II and I). Likewise, supernovae of these stars constantly enriched the interstellar medium with metals. Now, the interstellar medium in the Milky Way consists of about 32 % helium and traces of other metals (Danziger 1970).

Our Sun, a metal-rich Population I yellow dwarf star, emerged 4.6 billion years ago (Bahcall et al. 1995) from an accretion disk, formed by a collapsing rotating cloud. The compression within its center resulted in high temperatures, which initiated the fusion of hydrogen to helium (primarily pp chain reaction). The fusion reactions produce huge amounts of energy and heat the solar center to a temperature of 15.7 million kelvins (Christensen-Dalsgaard et al. 1996). The generated energy is transported through the solar body to its surface and eventually into space. The core region extends to about 0.25 solar radii ($R_\odot$), where the declining temperature becomes insufficient for fusion reactions. The energy transport is dominated by thermal radiation until, because of declining ionization and density, at 0.71 $R_\odot$ up to the surface convective motion takes over (Christensen-Dalsgaard et al. 1991).

The temperature at this transition region, called tachocline, is about 2 million kelvins and decreases up to the solar surface to between 4400–6600 K[3]. Here at the photosphere, the energy is radiated away with an effective black body temperature of 5772 K (Mamajek et al. 2015), classifying the Sun as a spectral type G2V star. At this surface layer, granules, the tops of convection cells, and temporary sunspots are visible. Strong magnetic flux inhibits the convection at sunspots, leading to lower temperature and brightness (for more on sunspots see the following Sections 2.2 and 2.3). Figure 2.1 illustrates these photospheric features along with the inner solar structure.

Above the photosphere at the base of the chromosphere, the temperature declines to its solar minimum of 3800 K until it raises to 2–3 million kelvins in the corona (Billings 1959; Liebenberg et al. 1975). Up to now it is not fully understood why the corona is so much hotter than the underlying chromosphere – this question is known as the coronal heating problem (Klimchuk 2006; McComas et al. 2007; Fox et al. 2015). The generally considered energy transfer mechanisms are magnetic reconnections, wave heating and type II spicules or a combination of these (Cranmer et al. 2017).

[1] ΛCDM: Lambda cold dark matter
[2] Percentages by mass.
[3] NASA Sun fact sheet: https://nssdc.gsfc.nasa.gov/planetary/factsheet/sunfact.html

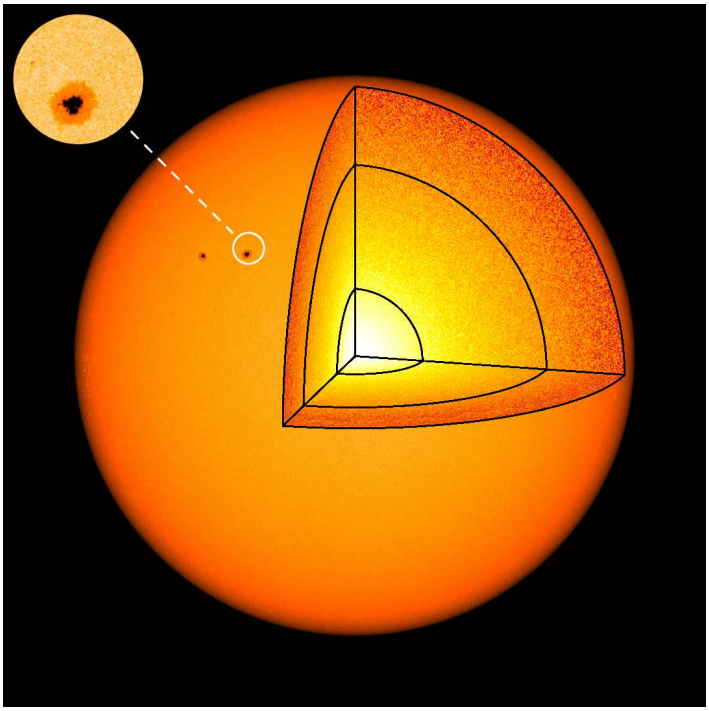

Figure 2.1 Image of the photosphere from 20 March 2016 together with a schema of the solar interior structure. The inset shows the granular surface with a sunspot. I created this figure based on a SDO/HMI continuum image, credit: NASA/SDO and the AIA, EVE and HMI science teams.

The chromosphere is a 2000 km thick region, whose features – numerous spicules, filaments, and prominences – can reach far into the corona. They consist of chromospheric material, channeled by the solar magnetic field, and are enveloped by a thin transition region where the temperature jumps up from about 30 000 K[4] to coronal temperatures. Reconnection of magnetic field lines can result in the eruption of filaments into the corona and beyond, termed coronal mass ejections (CMEs), see also Subsection 2.5.4. Details of chromospheric features are shown in Figure 2.2 – the images were taken on the same day as in Figure 2.1.

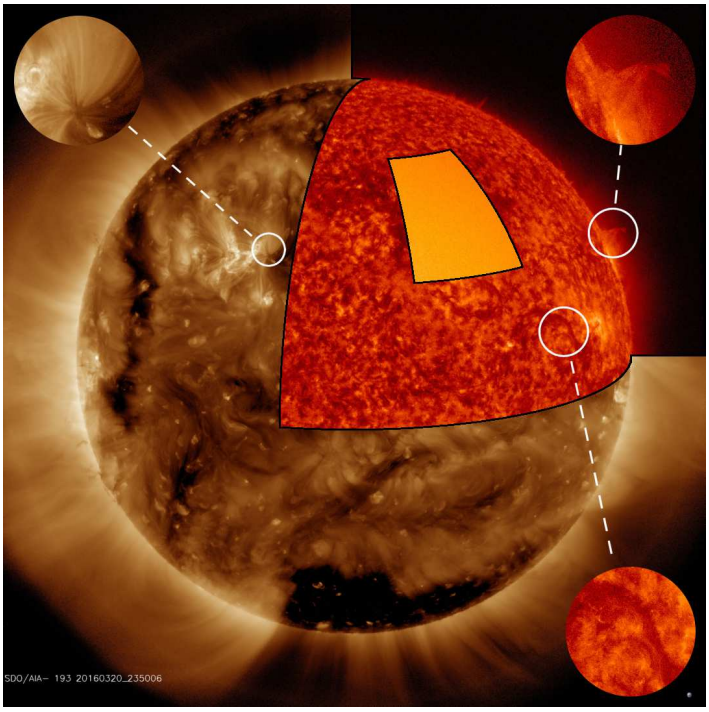

Figure 2.2 Composite image of the solar atmosphere from 20 March 2016 and some details of its features. Corona, chromosphere and photosphere are seen in wavelengths of 193 Å, 304 Å, and continuum. Chromospheric spicules are visible on the northern limb. The enlargements on the right show a prominence and a filament. The dark region at the south pole is a coronal hole. The left inset shows details of the active region belonging to the sunspots shown in Figure 2.1. I created this figure based on SDO/AIA images, credit: NASA/SDO and the AIA, EVE and HMI science teams.

The Sun's atmosphere is dominated by the varying small- and large-scale solar magnetic field configuration. There are regions where the magnetic field lines arc back to the surface and regions with open field lines. In the latter areas the coronal plasma can – guided by the field – escape into space. Thus, these coronal areas are less

[4]NASA Sun fact sheet: https://nssdc.gsfc.nasa.gov/planetary/factsheet/sunfact.html

dense, cooler and therefore appear darker in extreme ultraviolet (EUV) and are called coronal holes (CHs). In Figure 2.2 such a coronal hole is visible at the solar south pole.

From Earth, the faint corona and chromosphere can only be observed during eclipses, due to the brightness of the solar disk. There are three effects contributing to the visibility of the corona: photons scattering off free electrons, producing a continuous spectrum; photons scattering off dust particles, their spectrum contains Fraunhofer absorption lines; and ion spectral emission lines – these contributions to the corona are termed K-, F- and E-corona[5]. Images from solar eclipses reveal the coronal plasma, shaped by the magnetic field, and red prominences from the chromosphere. The solar eclipse imaged in Figure 2.3 shows the magnetic field's dipole structure and the equatorial streamer belt, characteristic for a quiet Sun during cycle minimum.

Figure 2.3 Total solar eclipse image of the inner corona up to a distance of five solar radii. The picture was taken in Mongolia, 1 August 2008 and is processed from multiple images. Credit: Miloslav Druckmüller, Peter Aniol, Jan Sládeček, 2008, reproduced with permission.

Due to the high coronal temperatures, plasma escapes the solar gravitational field (Parker 1958) with velocities of 200–800 km s^{-1}. Its acceleration is linked to the coronal heating – however, the exact location and process remain an open question (Hollweg 1985; McComas et al. 2007; Fox et al. 2015; Cranmer et al. 2017). The magnetic field becomes too weak to guide the coronal plasma at a distance of a few solar radii. From this so-called source surface, the solar wind flows radially outward into space until it reaches the termination shock. Eventually it collides with the local interstellar medium, creating the boundary of the heliosphere, the heliopause. The heliopause is expected to be a bubble of either teardrop or croissant shape, caused by the Sun's relative velocity of 23 km s^{-1} with respect to the local interstellar medium (Owens & Forsyth 2013; Opher et al. 2015). However, McComas et al. (2012) show that this velocity is too slow to form a leading bow shock. Measurements of the Voyager 1 and 2 spacecraft indicate their passage of the termination shock at about 94 au and 84 au, entering the heliosheath region (Owens & Forsyth 2013). Gurnett et al. (2013) report that in 2012 Voyager 1 actually crossed the heliopause into interstellar space at a solar distance of 121 au. The heliosphere and its surrounding flow structure is illustrated in Figure 2.4.

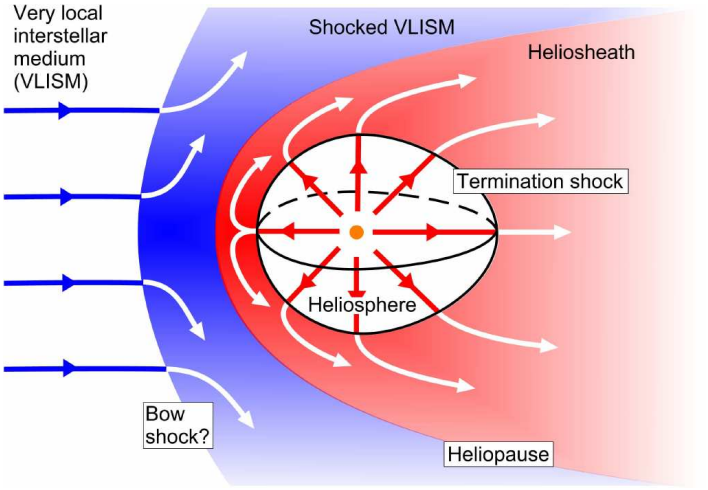

Figure 2.4 Schema of the heliosphere and its surrounding flow structure, formed by the interaction of the solar wind (red) with the local interstellar medium (blue) at the heliopause. Credit: Owens & Forsyth (2013, Fig. 9), licensed under CC BY-NC 3.0 DE.

On its way outwards through the solar system, the solar wind – carrying the solar magnetic field – interacts

[5] K from kontinuierlich (continuous in german), F from Fraunhofer, and E from emission.

with the planets, their magnetic fields and other solar system bodies. This has various effects, for instance disturbances in planetary magnetic fields with appearance of aurorae and enhanced radiation, atmospheric losses and stripping of cometary tails. Some of these effects can have disruptive consequences for humans and their technology, creating a high interest in understanding space weather and forecasting its effects, the topic of space weather is further addressed in Section 2.6. The magnitudes of these effects depend highly on spatial and temporal variations in the solar wind, which are rooted in the dynamics of the solar magnetic field, described in the following sections.

2.2 Solar dynamo

The conservation of the angular momentum in the contracting molecular cloud led to a rotation of the Sun. Although the Sun experiences a minor loss of angular momentum due to solar wind (Weber & Davis 1967), its rotation still has a current average period of about 25 days. The radial convective motion within the solar interior above the tachocline leads to a transport of momentum away from the rotation axis and therefore to a slower polar and faster equatorial rotation in the convection zone (Miesch 2005). This differential rotation is visible on the surface and was first discovered from sunspot observations by Scheiner (1630). With a rotation period of about 34 days, the poles have a lag of almost 9 days (for further information on solar rotation see appendix Section A.1). The differential rotation in the solar interior can be inferred from helioseismological observations. Below the differential rotation of the convection zone, a nearly solid rotation with a period of about 26.6 days (this corresponds to a frequency of 435 nHz) exists in the radiation zone, as shown in Figure 2.5.

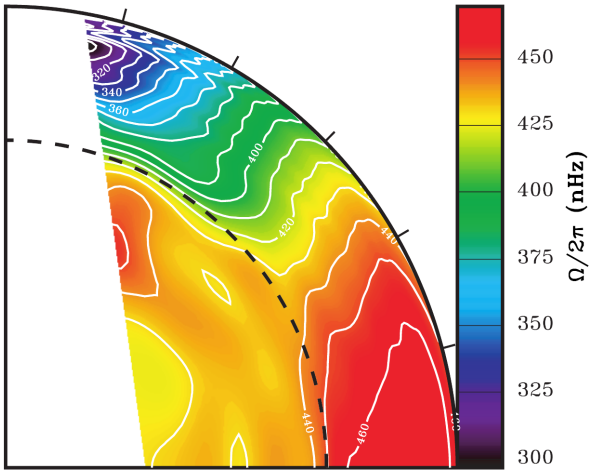

Figure 2.5 Rotation frequency profile of the solar interior. The location of the tachocline is indicated by the dashed line. The rotation frequency is inferred from helioseismology via observations from the Michelson Doppler Imager (MDI) at the Solar and Heliospheric Observatory (SOHO) spacecraft. Credit: Thompson et al. (2003, Fig. 3), © Annual Reviews, reproduced with permission.

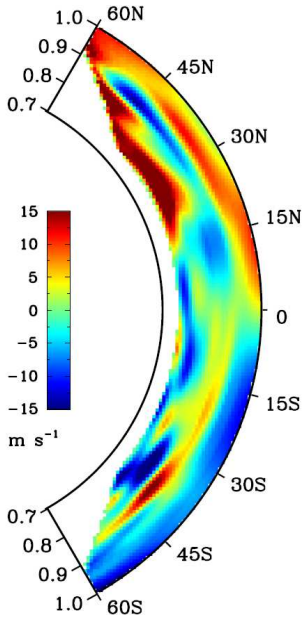

Figure 2.6 Meridional flow velocity profile in part of the convection zone. Positive values are directed towards north. The velocity is inferred from helioseismology via observations from the Helioseismic Magnetic Imager (HMI) at the Solar Dynamics Observatory (SDO) spacecraft. Credit: Zhao et al. (2013, Fig. 4, panel (a), I moved the colorbox), © AAS, reproduced with permission.

Turbulent plasma motions from convective flows in the convection zone generate and carry disorganized magnetic flux. The large rotational shear at the tachocline stretches and amplifies the magnetic fields to strong coherent toroidal flux (ω-effect) with intensities of the order 1–10 T. These toroidal fields, generated near the bottom of the convection zone, can be stored in a deep magnetic layer located in the stably stratified region below the convection zone (Ossendrijver 2003). The stronger flux ropes become buoyant and raise to the surface. The Coriolis force twists them systematically on their way through the convection zone (α-effect). The twist is stronger at higher latitudes (Joy's law). Then the flux ropes emerge in the photosphere as bipolar active regions of opposite magnetic polarity – the stronger ones forming pairs of sunspots, as seen in Figure 2.7.

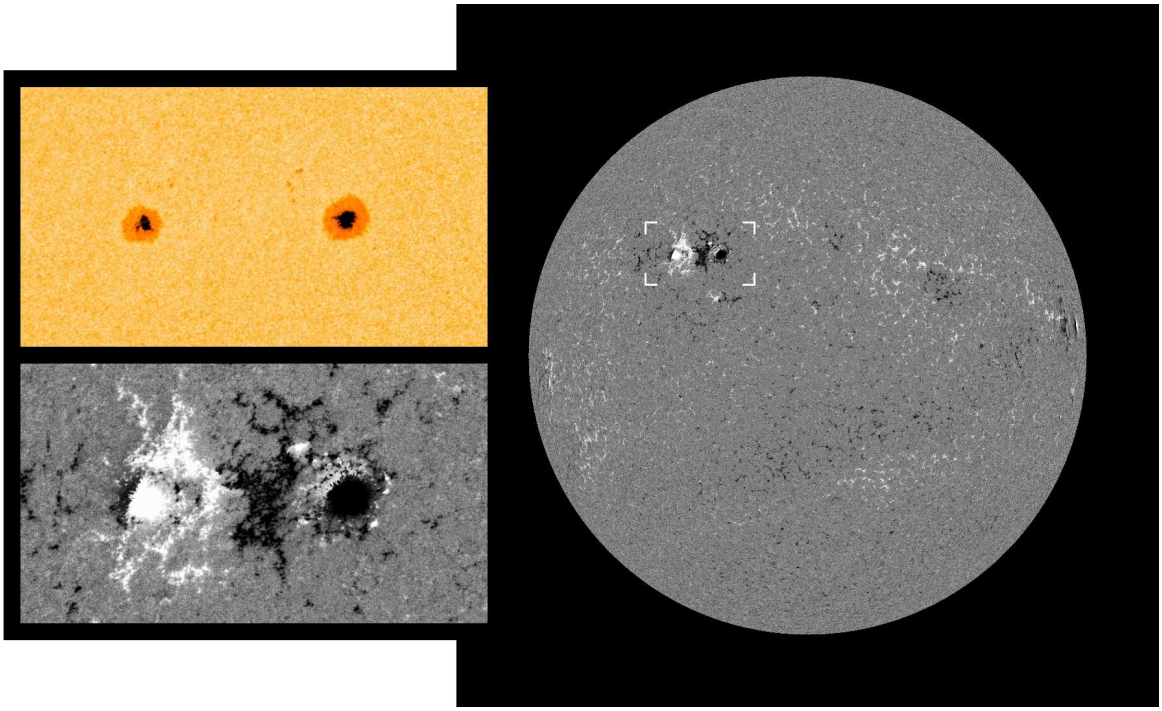

Figure 2.7 Continuum image of the two sunspots pictured in Figure 2.1 (top left), magnetogram from the same region (bottom left), and magnetogram from the whole solar disk (right). The magnetogram shows the polarity of the line-of-sight magnetic field component at the photosphere (black/white: inward/outward polarity). The highly concentrated magnetic flux at the sunspots is visible as well as the extended bipolar magnetic field structure of the whole active region, which is divided by the so-called magnetic neutral line. The solar disk is scaled to the same size as in Figure 2.1. I created the figure based on SDO/HMI continuum and magnetogram images from 20 March 2016, credit: NASA/SDO and the AIA, EVE and HMI science teams.

Turbulent convective diffusion of this surface flux contributes to the build-up of poloidal fields. Their resulting polarity is opposite to the prevailing global field due to the directional way the rotational shear at the tachocline and the Coriolis force in the convection zone act. Fluctuating motions further amplify the mean fields in these processes. This solar α-ω-dynamo is thought to create the major part of the solar magnetic field. Still, with regard to the magnetic field's high variability, the long-term mean fields are governed by intermittent localized structures, that is, active regions, filaments and coronal loops (Miesch 2005).

2.3 Solar activity cycle

Helioseismic measurements reveal that the large-scale convective flow is aggregated into large convection cells with slow meridional flows of a few $\mathrm{m\,s^{-1}}$, as can be seen from Figure 2.6. A poleward subsurface flow and equatorward backflow beneath with a further poleward flow below are detected within each hemisphere, comprising a stacked double-cell profile (Zhao et al. 2013). The meridional circulation flow speed has a major influence on the average 22-year period of the emerging magnetic flux at the solar surface, known as Hale cycle. This period varies and is influenced by the stochastic emergence rate and tilts of active regions and the diffusion from random convective motions (Hathaway & Upton 2016). The surface magnetic field configuration changes within one period from a dipole structure to a reversed dipole structure with opposite polarity and back, completing a so-called Babcock-Leighton dynamo cycle. Thus, the transition time from one dipole state to the next lasts about 11 years, this period is defined as one solar cycle.

In the transition phase, magnetic flux emerges in belts above and below the solar equator, manifesting as bipolar active regions with sunspots, resulting in a toroidal/multipolar structured magnetic field. Sunspots appear at about $\pm 20°$ latitude at the beginning of a cycle, this shifts towards lower latitudes at the end of a cycle. Thus, the plot of sunspots over latitude and time reveals a butterfly pattern (Maunder 1904). This butterfly pattern appears in surface radial magnetic field observations as well, see Figure 2.8. The leading polarity of bipolar regions is opposite in both hemispheres and the leading polarity changes with each solar cycle, this is called Hale's polarity law. The emerging flux is carried by the slow meridional surface flow poleward, canceling the current dominating polar field polarity and eventually resulting in the polar field switch

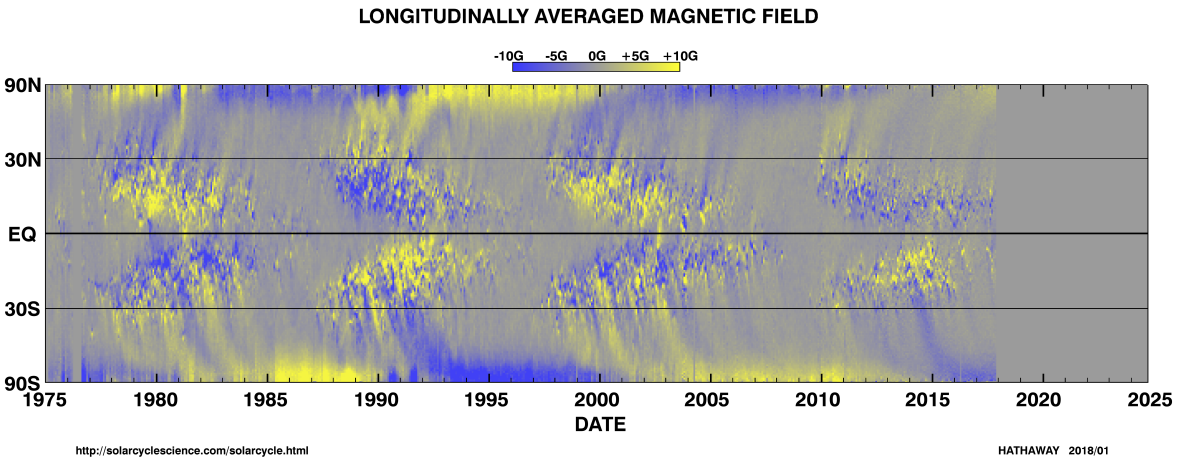

Figure 2.8 Magnetic butterfly diagram of the longitudinally averaged radial magnetic field on the solar surface. Yellow represents an outward directed magnetic field (positive), blue inward (negative). The data is obtained from instruments on Kitt Peak National Observatory and from the MDI at the SOHO spacecraft. Courtesy of David Hathaway, Solar Cycle Science, 2018, updated version of Hathaway (2015, Fig. 17).

(Hathaway 2015).

Since regions of strong magnetic flux are visible as sunspots on the photosphere, they were known well before the common era by greek and chinese scholars (Clark & Stephenson 1978; Vaquero 2007). Systematic sunspot observations exist since 1610, shortly after the invention of the telescope. In 1843 Schwabe discovered the 11-year periodicity in the sunspot occurence (Schröder 2004, p. 124). In 1848 Wolf introduced the sunspot number (SSN) and the solar cycle number to record these cycles (Hathaway 2015). The SSN observations, see Figure 2.9, show large variations in cycle length (9–14 years) and cycle amplitude, with peak SSNs in the range 0–300, (Hathaway 2015). There also exist long-term variations, such as secular cycles of different

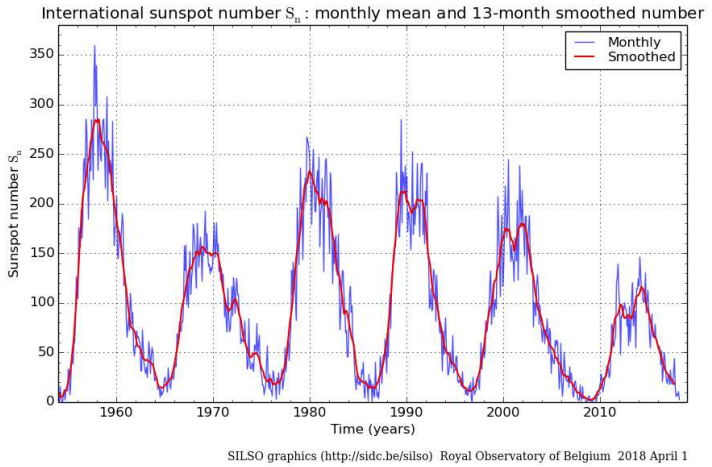

Figure 2.9 Monthly mean sunspot number (blue) and 13-month smoothed monthly sunspot number (red) since 1954. Credit: SILSO data/image, Royal Observatory of Belgium, Brussels, 2018.

periodicity or the 70-year Maunder Minimum, during which from 1645 on almost no sunspots were observed, (Maunder 1890). The source of the variations in the solar cycle periods and amplitudes are variations in the meridional circulation, because their fluctuations are larger than those found in the differential rotation and in the convective motions (Hathaway 2015).

As the SSN is commonly used as an indicator for solar activity, there exists interest in its prediction for the course of the actual and upcoming solar cycles. The continuing prediction of an already commenced activity cycle is reliable, but then the prediction of a cycle before it began is more difficult. Though, there are indications that the polar magnetic field strength during the preceding activity minimum is correlated to the strenght of the next solar cycle (Schatten & Sofia 1987). However, Hathaway & Upton (2016) suggest that the predictability of solar cycles is generally limited – accumulated uncertainty produced by stochastic motions in the convection zone makes predicitons further than the next solar cycle very unreliable.